

# Fast Geolocation for Hot Spot Detection \*

E. Salamí, C. Barrado, M. Pérez-Batlle, P. Royo, E. Santamaria, E. Pastor<sup>a</sup>

Technical University of Catalonia, 08860 Castelldefels, SPAIN – [esalami@ac.upc.edu](mailto:esalami@ac.upc.edu)

**Abstract** – In this paper we present an algorithm for fast geolocation of hot spots from an infrared image taken from an unmanned aircraft. The input data are the position and attitude of the aerial platform, and the digital elevation model of the terrain. The down faced orientation of the camera and the stable flight of the aircraft contribute to reduce the number of floating point operations needed for geolocation. These simplifications will result on an increase of the accumulated errors, added to those of the measuring instruments. In the paper we will compare the geolocation results of the complete computational model with the proposed fast model.

**Keywords:** Forest fire, Photogrammetry, Vision, Airborne In situ Measurements, UAS

## 1. INTRODUCTION

Wild fires are a devastating catastrophe for forest, especially in Mediterranean countries. More than 50,000 fires are detected in South Europe each year which burnt from 200,000Ha in the 'good' years to more than 750,000Ha in the worst recent year (2003). Much effort is done today in prevention, detection and extinction tasks. In terms of costs, extinction represents the 70% of the total budget of the firemen. Supporting the decision making process might improve the effectiveness of the dedicated resources.

Remote Sensing is the process of acquiring, processing and interpreting the electromagnetic waves of an area from an aerial mean. Traditionally satellites have been the main source of Remote Sensing data. Increasing number of constellations and better precision had driven many qualified studies, mainly for scientific use. In the case of wild fires, studies on the behavior of past fire fronts made possible the simulation on new fires, thus the anticipation of fire fronts movement. Another approach for Remote Sensing is the use of aircrafts. Aircrafts are used today to obtain more precision data of a given region.

Unmanned Aerial Systems (UAS) are promising technology for remote sensing, specially for tactical reaction in emergency situations. In forest fire scenarios, we propose the use of a UAS with an infrared camera down faced to locate hot spots. For the low altitudes of a UAS, COTS cameras are good enough to obtain good quality images (Dunagan, 2005).

The UAS is controlled by an autopilot enlarged with new flight capacities. In particular, area scan pattern is the flight trajectory proposed for the complete area surveillance. In such pattern the UAS flies parallel trajectories back and forth, capturing images of the whole area. The turning maneuver is done outside of the area, thus the UAS flight is stable (roll and pitch angles are zero) when images are captured. A fast search on the infrared image finds the pixel locations of the

hot spots. The computation of the geographic location of the hot spot is rapidly needed in order to inform ground crew.

This paper presents the algorithm implemented in the UAS for the fast geolocation of the hot spots found in the infrared image. The inputs of the algorithm are the camera constants (focal length, sensor pitch and pixel resolution), the aircraft telemetry (location and attitude), and the digital elevation model of the terrain. The output of the algorithm is the geolocation of the hot spot. A similar work is applied to manned aircraft in (Wright, 2004) but not considering the terrain slopes.

For a fast computation we fix the orientation of the camera to be down faced. We also assume a stable flight of the aircraft. Both assumptions contribute to reduce the number of floating point operations needed for geolocation. But they also will result on an increase of the location error, added to those of the measuring instruments, computations or terrain data. The paper measures the errors of the geolocation results and cost differences of their computation between the complete computational model and the proposed fast model. Then, in order to reduce mistakes due to the geolocation errors, we propose to fusion (Shokr, 2000) visual and thermal images for human observers.

The paper is organized as follows: Section 2 presents previous works and the existing geolocation algorithms. Section 3 presents our architecture, provides the details of our light implementation of geolocation and shows the results of its execution. Finally in Section 4 conclusions and future work are given.

## 2. GEOLOCATION ALGORITHMS

Geolocation is the task of identifying the geographic coordinates of some target. In our case, we want to find the coordinates of a hot spot found in a thermal picture obtained from a UAS.

Similar works have been presented previously. Some consider the elevations of the terrain (Sheng 2005, Johnston 2006), but many of them do not consider the terrain, but only the attitudes of the airframe and of the camera. In such cases geolocation consists basically in using matrix rotation to transform coordinates systems (McGlone, 2004).

For example (Wright, 2004) used a precise positioning system (with inertial sensors and differential GPS) on board a manned aircraft to obtain thermal images at 400m altitude. Their algorithm was able to locate hot spots in real time with 10m accuracy. (Barber, 2006) applied also geolocation without considering terrain slopes using a UAS with a gimbaled camera. After matrix rotations they also apply recursive least square filtering to the image sequence to improve accuracy up to 3m with no differential GPS. Also a

---

\* This work has been partially supported by Spanish Ministry of Education under contract TIN2010-18989 and by AGAUR under contract VALTEC-09-2-0099.

UAS was used in (Zhou, 2010) with differential GPS precise position and a video camera. The accuracy they obtain was 2m for 200m altitude flights.

Other works are more devoted to study the effects of terrain elevation and slopes in geolocation. The Digital Elevation Model (DEM) is a raster file with the mean elevation of the terrain cell it represents. (Johnston, 2006) presents a geolocation algorithm for video images taken from a UAS using a 1x1km DEM, thus considering a semi flat Earth. But typical cell sizes today are 90x90m and 30x30m. Geolocation consist then in finding the intersection of the single ray pointing to the target with the plane of the terrain obtained from the DEM.

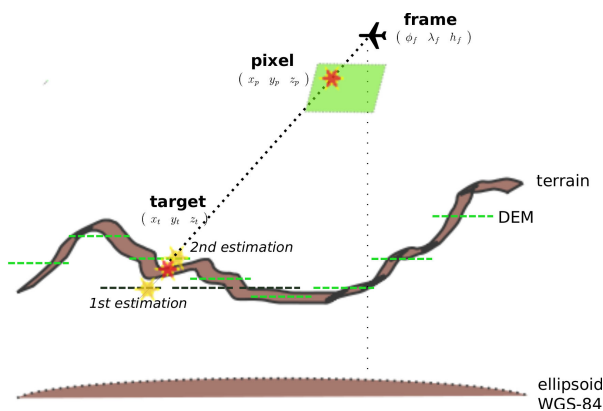


Figure 1. Geolocation

Figure 1 shows the involved concepts. The UAS (or more generally, any air frame) is flying and takes a picture in a given moment. The picture is tagged with the telemetry of the UAS, this is, its location and its attitude. The location of the UAS is defined as latitude  $\phi_f$ , longitude  $\lambda_f$  and height  $h_f$ , considering height above ellipsoid WGS-84.

The algorithm for target geolocation using the DEM is an iterative loop that approximates the coordinates of the target using triangulation. On each iteration, a new estimated elevation of the target is obtained from the DEM raster data. Initially the terrain elevation of the target is estimated as the terrain elevation in the vertical (z axis) of the air frame. Every iteration computes the intersection of the ray line with the estimated elevation plane. With the intersection coordinates a new estimated value of the terrain elevation is obtained for the new iteration. The loop finishes when the estimated terrain altitude is repeated. (Sheng 2005) proposes this iterative algorithm and studies the results on variety of slope surfaces. They proved that the method converges when slope angles are smaller than the angle formed by the incident ray and the ground.

### 3. IMPLEMENTATIONS AND RESULTS

This section describes the distributed architecture on board the UAS designed for the hot spot mission, details our algorithm for geolocation and presents the sources of errors introduced with our simplification.

#### 3.1 UAS software architecture

We base our architecture in the Service Oriented Architecture (SOA) paradigm: Functionalities are deployed into independent software elements, called services. Services communicate with each other with a publish-subscribe model. The published data is broadcast to a common network and any service can subscribe.

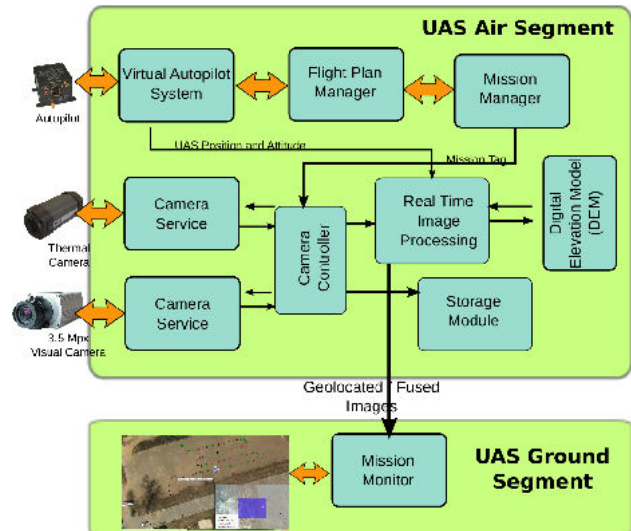


Figure 2. Services for the Sky-Eye mission

A set of available services have been already implemented to give support to most types of remote sensing UAS missions. They provide useful functionalities which simplify the development of the UAS hot spot mission. Figure 2 illustrates the main services involved. At the left side of the figure and connected with the autopilot, the virtual autopilot service is designed to hide the specificities of the selected autopilot. This service virtualizes the access to the flight capacities. It works in conjunction with the flight plan manager, a service that translates dynamically complex flight profiles into autopilot orders. These two services, together with the autopilot, form the stack of the flight capacities of the UAS, from a flight plan file with high semantics to the low semantics of the UAS maneuvers. Two flight monitoring services reside on ground for pilot control, but are not showed in this figure.

Mission manager and mission monitor are in charge of executing the mission under the supervision of the operator. They organize the activities and flow information of the mission: Photographies are taken upon mission manager requests through the camera controller. At the beginning of the mission this service configures the two cameras issuing messages to the camera services and subscribes to the pictures and to the telemetry. Then, for each image being published on the system, the camera controller receives it and associates the aircraft position. The georeferenced images are then subscribed by real time data processing services and by the storage module.

The image processing service analyses the thermal images looking for hot spots. When found, it is in charge of georectifying the image, using matrix rotations as explained

in (McGlone 2004) and generates an event with the hot spot pixel coordinates and temperature.

### 3.2 Algorithm

Being  $p[m, n]$  the coordinates of pixel corresponding to the hot spot center of mass in the thermal image, and  $(\varphi_p, \lambda_p, h_p)$  the geodetic coordinates of the UAS, the base iterative algorithm computes the target coordinates, first Cartesian  $(x_p, y_p, z_p)$  and then geodetic  $(\varphi_t, \lambda_t, h_t)$ . Listing 1 formalizes the algorithm.

```

(xp, yp, zp) = NED coordinates (ρ[m,n])
ht = DEM (ϕp, λp)
while (ht is new)
  xt = (hf - ht) xp / zp
  yt = (hf - ht) yp / zp
  zt = (hf - ht)
  (ϕt, λt) = Geodetic coordinates (xt, yt, zt)
  ht = DEM (ϕt, λt)
done

```

Listing 1. Iterative algorithm

Starting from the terrain elevation on the vertical of the air frame position, the algorithm approximates the coordinates of the target in an iterative loop. For each assumed terrain altitude,  $h_t$ , the new target coordinates are computed as the intersection of the ray line and the elevation plane. Equations of the ray line and the elevation plane are given in North-East-Down (NED) system with origin at the aircraft center of gravity.

The first operation is the conversion of the pixel coordinates  $(m, n)$  into NED coordinates  $(x_p, y_p, z_p)$ . Then the loop applies triangulation to obtain the Cartesian coordinates of the target, and converts them into geodetic coordinates because the DEM data is given only for longitude and latitude.

The algorithm has been tested for geolocating all the pixels of an image taken for a steep terrain. The results showed that the mean number of iterations needed until converging to the target location was 1.8. The number of floating point operations of the iterative algorithm are given in table 1. The computation for obtaining the pixel NED coordinates has to be done only once, but it is an expensive operation, needing up to 165 floating point operations, mainly products. The operations inside the loop are not so expensive (69) and represent for the 1.8 iteration mean, about the 40% of the cost of the algorithm. In our fast algorithm we are going to simplify the pixel NED coordinates calculation. In (1) you can see the details.

Given the aircraft navigation angles yaw, pitch and roll  $(\psi, \theta, \varphi)$ , the camera orientation angles pan, tilt and roll  $(\omega, \alpha, \rho)$  and the camera internal parameters pixel pitch, pixel resolutions and focal length  $(S, M, N$  and  $f)$ , the first expression shows the full conversion model. In our fast version (2) we assume that the camera is down faced (tilt angle  $\alpha=0$ ) and that the airframe is flying stable (pitch  $\theta$  and roll  $\varphi$  angles are also 0) thus the differences of the computations needed is very significant: After the simplification the number of floating point operations for having the pixel NED coordinates is reduced from 165 to only 14. For the 1.8 mean number of iterations, this is a 58% reduction of the number of floating point iterations. The average elapsed time needed for the fast geolocation of one pixel was 0.13ms.

$$\begin{pmatrix} x_p \\ y_p \\ z_p \end{pmatrix}_{(\theta, \varphi, \psi)} = \begin{pmatrix} \cos \psi \cos \theta & -\sin \psi \cos \theta & \cos \psi \sin \theta \sin \varphi & \sin \psi \sin \theta \sin \varphi & \cos \psi \sin \theta \cos \varphi \\ \sin \psi \cos \theta & \cos \psi \cos \theta & \sin \psi \sin \theta \sin \varphi & -\cos \psi \sin \theta \sin \varphi & \sin \psi \sin \theta \cos \varphi \\ -\sin \theta & \cos \theta & \cos \psi \sin \varphi & \sin \psi \sin \varphi & \cos \theta \cos \varphi \end{pmatrix} \begin{pmatrix} m \\ n \\ 1 \end{pmatrix}$$

$$\begin{pmatrix} x_p \\ y_p \\ z_p \end{pmatrix}_{(\theta, \varphi, \psi)} = \begin{pmatrix} \cos \omega \cos \alpha & -\sin \omega \cos \alpha & \cos \omega \sin \alpha \sin \rho & \sin \omega \sin \alpha \sin \rho & \cos \omega \sin \alpha \cos \rho \\ \sin \omega \cos \alpha & \cos \omega \cos \alpha & \sin \omega \sin \alpha \sin \rho & -\cos \omega \sin \alpha \sin \rho & \sin \omega \sin \alpha \cos \rho \\ -\sin \alpha & \cos \alpha & \cos \omega \sin \rho & \sin \omega \sin \rho & \cos \alpha \cos \rho \end{pmatrix} \begin{pmatrix} m \\ n \\ 1 \end{pmatrix}$$

$$\begin{pmatrix} x_p \\ y_p \\ z_p \end{pmatrix}_{(\theta, \varphi, \psi)} = \begin{pmatrix} -S & 0 & T_x \\ 0 & S & -T_y \\ 0 & 0 & f \end{pmatrix} \begin{pmatrix} m \\ n \\ 1 \end{pmatrix}$$

(1)

$$\begin{pmatrix} x_p \\ y_p \\ z_p \end{pmatrix}_{(\theta, \varphi, \psi)} = \begin{pmatrix} \cos \psi & -\sin \psi & 0 \\ \sin \psi & \cos \psi & 0 \\ 0 & 0 & 1 \end{pmatrix} \begin{pmatrix} -S & 0 & T_x \\ 0 & S & -T_y \\ 0 & 0 & f \end{pmatrix} \begin{pmatrix} m \\ n \\ 1 \end{pmatrix}$$

(2)

Where

$$T_x = S(M-1)/2$$

$$T_y = S(N-1)/2$$

### 3.3 Sources of error in Geolocation

We detail three sources of errors: the aircraft position inaccuracy, the digital representation of the terrain elevation (known as planimetric representation) and the attitude error that we introduce by assuming a stable flight and a down faced camera. All three errors are shown in Figure 3. We do not consider camera distortions or blooming effects on the hot spot thermal image.

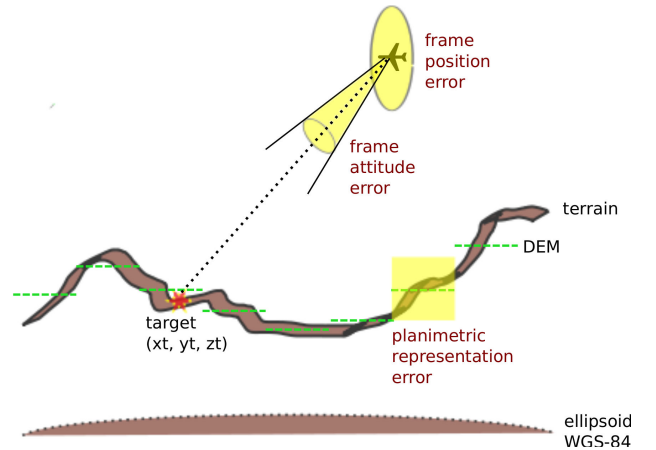


Figure 3. Inaccuracies that influence the target location

The frame position error is basically coming from the GPS signal inaccuracies. These have improved from 1990 having now errors around 5m in the horizontal position and 10m on the vertical (Leva, 1996). The projection of such error on air into the terrain depends on the attitude angle and the camera aperture angle. The best cases are given for  $0^0$  attitude angle and the narrowest aperture angle of the camera. In any case for angles smaller than  $45^0$  the final error in the terrain is always lower than the aerial error, this is less than 15m (5 horizontal + 10 vertical).

The DEM planimetric error has also some influence on the terrain location error. The size of the DEM cells is very significant in the final accuracy of the elevation vertical error. For DEM with 30x30m cells the estimated errors are usually in the 5 to 10m. The projection of such errors into the geolocation algorithm depends also on the attitude angle. But again for angles lower than  $45^0$  the final error is less than the DEM error.

Finally, for the attitude error pitch and roll actual values are very influent. Figure 4 shows them measured during a helicopter test flight. The values are in a range from  $-16^{\circ}$  to  $12^{\circ}$  and have not correlation. (Zhou, 2010) measured the roll and pitch angles and obtain similar figures than our test flight.

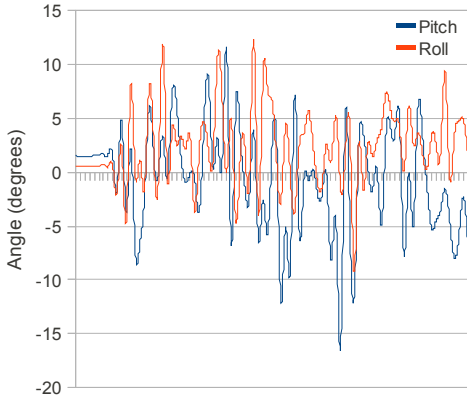


Figure 4. Pitch and roll angles on a test flight

In the table 2 we show the error values for attitude angles up to  $20^{\circ}$ . We give values for low altitude flights: 50m, 100m, 150m, 200m and 250m. As expected the higher the altitude of the aircraft, the larger the error is. But attitude error values are in the same order of magnitude than position errors and planimetric errors. If we can synchronize the picture shot with a stable attitude (i.e. bellow the  $5^{\circ}$  angle) errors introduced will not be significant for the hot spot mission.

error (m)	5	10	15	20 Attitude (deg)
50	4,37	8,82	13,40	18,20
100	8,75	17,63	26,79	36,40
150	13,12	26,45	40,19	54,60
200	17,50	35,27	53,59	72,79
250	21,87	44,08	66,99	90,99

Table 2. Accuracy errors variability with altitude and attitude

#### 4. CONCLUSIONS

This paper presents the use of an Unmanned Aerial System for Remote Sensing in the particular scenario of hot spots detection. UAS provide significant advantages in front of current alternative systems in terms of flexibility, precision, cost, and safety. The system performs real time processing of pictures taken with a thermal camera and applies a simple threshold algorithm to detect hot spots. Then, to geolocate the hot spot, typical algorithms use the UAS position, UAS attitude and pixel coordinates. We showed that assuming a stable flight and having a fixed down faced camera, a 58% reduction of the floating point operations can be achieved. A mean elapsed time of 0.13ms shows the possibility of using this algorithm in real time. But 70% of the time is devoted to reading DEM data. To improve geolocation speed a new strategy for DEM access should be investigated.

(Barber, 2006) quantified the final geolocation horizontal error in 20-40m. The error introduced by our algorithm is shown to be in the same orders of magnitudes. For

overcoming the location errors with low cost equipments we propose to provide the end users with visual images of the environment fused with the hot spot thermal information.

#### REFERENCES

D. Barber, J. Redding, T. McLain, R. Beard, and C. Taylor, "Vision-based Target Geo-location using a Fixed-wing Miniature Air Vehicle", *Journal of Intelligent and Robotic Systems*, 47 (4): 361-382, Dec 2006.

S. Dunagan, D. Sullivan, R. Slye, B. Lobitz, E. Hinkley, and S. Herwitz, "A Multi-Sensor Imaging Payload for Mission-Adaptive Remote Sensing Applications" *AIAA Infotech@Aerospace*, Arlington, VI, Sep 2005.

M.G. Johnston, "Ground Object Geo-Location using UAV Video Camera", *25th Digital Avionics Systems Conference*, 2006 IEEE/AIAA, pp. 1-7, Oct 2006.

J.L. Leva, "An alternative closed-form solution to the GPS pseudo-range equations", *IEEE Transactions on Aerospace and Electronic Systems*, 32 (4): 1430-1439, Oct 1996.

J.C. McGlone, E.M. Mikhail, and J.S. Bethel, "Manual of Photogrammetry", *American Society on Photogrammetry and Remote Sensing*, 2004.

Y. Sheng, "Theoretical Analysis of the Iterative Photogrammetric Method to Determining Ground Coordinates from Photo Coordinates and a DEM", *Photogrammetric Engineering & Remote Sensing*, 71 (7): 863-871, 2005.

M. Shokr, "Remote sensing data fusion by co-location of footprints from different sensors", *Geoscience and Remote Sensing Symposium, IGARSS 2000*, Vol. 6, pp. 2432, Honolulu, 2000.

D. Wright, T. Yotsumata, N. El-Sheimy, "Real time identification and location of forest fire hotspots from geo-referenced thermal images". *International Archives of Photogrammetry Remote Sensing and Spatial Information Sciences*, 35 (2), 13-18, 2004.

G. Zhou, "Geo-Referencing of Video Flow from Small Low-Cost Civilian UAV", *IEEE Transactions on Automation Science and Engineering*, 7 (1): 156-166, Jan 2010.